Electronic Supplementary Information (ESI)

Strong increase in the effective two-photon absorption cross-section of excitons in quantum dots due to the nonlinear interaction with localized plasmons in gold nanorods

Victor Krivenkov,*[a] Pavel Samokhvalov,[a] Ana Sánchez-Iglesias,[b] Marek Grzelczak,[c,d] Igor Nabiev[a,f] and Yury Rakovich**[c,d,e,g]

[a]National Research Nuclear University MEPhI (Moscow Engineering Physics Institute), 31

Kashirskoe shosse, 115409 Moscow, Russian Federation

[b]CIC biomagune, Paseo de Miramón 182, 20014 Donostia - San Sebastián, Spain

[c]Centro de Física de Materiales (MPC, CSIC-UPV/EHU), Paseo Manuel de Lardizabal 5, 20018

Donostia - San Sebastián, Spain

[d]Donostia International Physics Center (DIPC), Paseo Manuel de Lardizabal 4, 20018

Donostia-San Sebastián, Spain

[e]Departamento de Física de Materiales UPV-EHU, Paseo Manuel de Lardizabal 5, 20018

Donostia-San Sebastian, Spain

[f]Laboratoire de Recherche en Nanosciences (LRN-EA4682), Université de Reims Champagne-

Ardenne, 51100 Reims, France

[g]IKERBASQUE, Basque Foundation for Science, Maria Diaz de Haro 3, 48013 Bilbao, Spain

Contact authors: *vkrivenkov@list.tu and **yury.rakovich@ehu.eus

1. Sample synthesis and preparation

1.1 Materials.

Cadmium oxide (99.5%, powder), cadmium acetate dihydrate (98%), 2-ethylhexanoic acid (2-EHA, 99%), myristic acid (MA, ≥99%), oleic acid (≥99%), 1-octadecene (ODE, technical grade, 90%), oleylamine (OLA, technical grade, 70%), hexadecylamine (technical grade, 90%), trioctylamine (TOA, 98%), trioctylphisphine (TOP, technical grade, 97%), selenium powder (powder, 100 mesh, 99.5%), zinc oxide (puriss, 99–100%), thiourea (TU, ACS Reagent, >99%),

triethylene glycol dimethyl ether (TEGDME, 99%) were purchased from Sigma-Aldrich. n-Hexadecylphosphonic acid (97%) was purchased from PlasmaChem GmbH. Methyl acetate (extra pure, 99%) was purchased from Acros. Hexane, n-decane, toluene, methanol, and isopropyl alcohol of spectroscopy grade were purchased from the local supplier Ekos-1. All reagents were used as received without purification.

Preparation of cadmium myristate. 14 mmol of CdO, 42 mmol of MA and 50 mmol of n-decane were placed into a 100-ml round-bottom flask equipped with a reflux condenser. This mixture was gently heated at a low stirring rate until refluxing started, and then it was kept at this temperature for 2 h until all cadmium oxide was dissolved. This hot solution was slowly poured into a beaker containing 400 of methanol (Caution! Boiling of methanol may occur) to obtain a white gelous precipitate containing a mixture of cadmium myristate and unreacted MA. After the thermal equilibrium was reached, the beaker was heated on a hotplate to 55°C under mild stirring to dissolve unreacted MA in the methanol phase, and the precipitate was vacuum-filtered. The product collected on the glass filter was washed three times with 60 ml of cold methanol, dried with an air flow, and transferred into a beaker containing 100 ml of hexane. At this stage, which is necessary to remove the decane residue entrapped during the first precipitation, the mixture was heated until hexane started boiling, and the loose precipitate was collected by the second filtration under reduced pressure. Finally, the obtained product was dried under vacuum to obtain 6.4 g of cadmium myristate (the reaction yield was 81%).

Preparation of shell precursor solutions. The Zn precursor solution was prepared by dissolution 30 mmol of zinc oxide in a 2.05-fold excess of 2-EHA dissolved in 40 ml of ODE. This procedure was performed at 120°C in an Ar atmosphere under mild stirring. When all ZnO was completely dissolved, the clear solution was cooled down to 60°C, transferred to a 50-ml volumetric flask, and leveled with a small portion of ODE to obtain a 0.6 M Zn precursor solution. The cadmium precursor solution (0.4 M) was obtained in a similar way, except for the dissolution, which was performed at a higher temperature of 160°C. The sulfur precursor was obtained by sonication of

42.7 mmol of thiourea in 40 ml of TEGDME for 1 h. After the sonication, the precursor solution was leveled by another portion of TEGME in a 50-ml volumetric flask to obtain a 0.85 M sulfur precursor solution. All precursor solutions were stored before use in the dark at room temperature.

1.2 CdSe (core) / ZnS/CdS/ZnS (multishell) quantum dots

The details of the synthesis of CdSe/ZnS/CdS/ZnS core/multishell QDs have been published by us before.[S1] Briefly, 2.3-nm CdSe core nanocrytals were obtained by the hot injection synthesis using cadmium hexadecylphosphonate and trioctylphosphine selenide (TOPSe) as the sources of Cd and Se, respectively. Injection of a cold TOPSe solution into a hot Cd precursor solution was performed at 240°C, the reaction was allowed to proceed for 5 min at 230°C, after which the core nanocrystal solution was rapidly cooled using an intense flow of air. CdSe nanocrytals were isolated from the reaction solution by precipitation with excess of methyl acetate and subsequent centrifugation. The nanocrytal pellet left at the bottom of the centrifuge tube was dissolved in toluene, and an aliquot containing 100 nmol of CdSe nanocrystals with the 2.3-nm core diameters (determined from the optical absorbance spectroscopy)[S2] was transferred into a shell growth solution consisting of 3 ml of ODE and 3 ml of OLA. The complex ZnS/CdS/ZnS muthishell was grown using the alternate precursor injection procedure known as SILAR[S3]. The exact quantities of the precursors required for deposition of strictly one-monolayer-thick shell layers were determined using atomistic simulation of the QD structure, which will be described elsewhere, but these could be roughly estimated by a 30% reduction of the values obtained from the spherical shell model as described[S3]. The deposition of individual shell layers was performed at 170°C for ZnS shells and 160°C for CdS shell. After the reaction was completed, the core/multishell QD solution was cooled down to room temperature and transferred into a centrifuge tube. Nanocrystals were precipitated by a twofold volume excess of the methyl acetate. After centrifugation at 5 000 rpm, the clear supernatant was discarded and the compact QD pellet was dissolved in 10 ml of hexane and stored in the dark before use. The obtained QDs (Fig. S1) had a uniform shape and a mean diameter of 4.57 ± 0.47 nm.
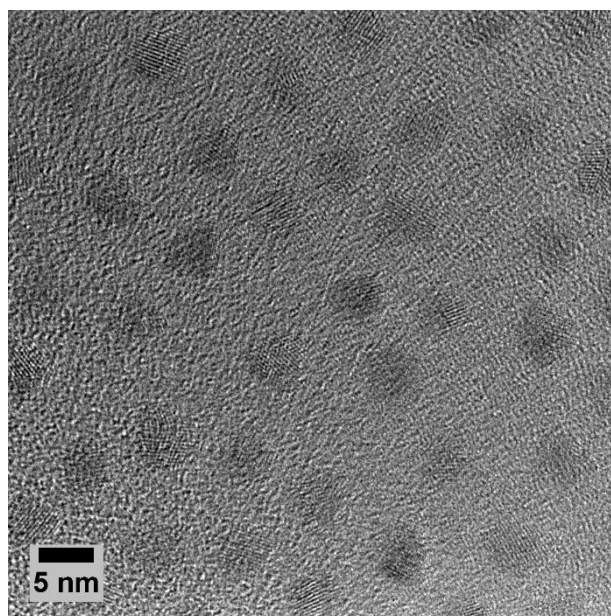
Fig. S1. TEM image of CdSe/ZnS/CdS/ZnS core/multishell quantum dots.

1.3 Gold nanorods

Tetrachloroauric acid (HAuCl$_4$), sodium borohydride (NaBH$_4$), hexadecyltrimethylammonium bromide (CTAB), benzyldimethylhexadecylammonium chloride (BDAC), silver nitrate (AgNO$_3$), hydrochloric acid (HCl), ascorbic acid (AA) were purchased from Sigma-Aldrich. Gold nanorods were prepared using Ag-assisted seeded growth. Seeds were prepared by the reduction of HAuCl$_4$ (5 mL, 0.25 mM) with NaBH$_4$ (0.3 mL, 10 mM) in aqueous CTAB solution (100 mM). An aliquot of seed solution (0.12 mL) was added to a growth solution containing CTAB (50 mL, 100 mM), HAuCl$_4$ (0.5 mL, 50 mM), ascorbic acid (0.4 mL, 100 mM), AgNO$_3$ (0.6 mL, 10 mM) and HCl (0.95 mL, 1000 mM). The mixture was left undisturbed at 30 ºC for 2 h. The solution was centrifuged twice (8000 rpm, 30 min) and redispersed in BDAC (10 mM) to obtain a final concentration of gold equal to 0.25 mM. The TEM image of the gold nanorods is in the Fig. S2.
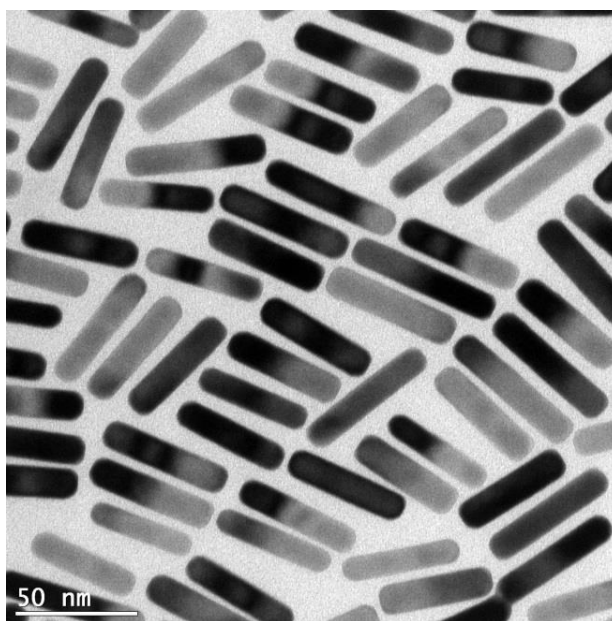
Fig. S2. TEM image of gold nanorods

2. Measurements of the photoluminescence intensity and lifetime

The PL signals were measured using a femtosecond laser luminescent setup based on a Tsunami femtosecond laser (Spectra Physics) with a pulse repetition rate of 80 MHz, tunable pulse duration of up to 60 fs, and pulse energy of up to 20 nJ (Fig. S3). Additionally, a laser pulse selector module (Model 3980-6M, Spectra Physics) was used to reduce the pulse repetition rate to 1.6 MHz in the case of time-resolved measurement; however, this module also reduced the pulse duration to 300 fs and pulse energy to 4 nJ per pulse. The PL signal was excited and collected by a confocal optical scheme using a lens with a focusing length of 35 mm (or 80 mm in some cases). The PL signal was recorded by means of a M266 monochromator/spectrograph (Solar Laser Systems) with a Hamamatsu high-sensitivity CCD module installed. A PD-050-CTD (Micro Photon Devices) detector with a resolution of up to 50 ps connected to a Pico Harp 300 electronic photon counting module (Pico Quant) was additionally connected to the monochromator/spectrograph to measure the PL decay kinetics by the method of time-correlated single-photon counting. The setup allowed PL time-resolved measurement with a time resolution of down to 150 ps. We tuned the pulse energy using a polarizing laser pulse attenuator, dividing the laser beam into two (p-polarized and s-polarized beams). We used only the p-polarized beam.
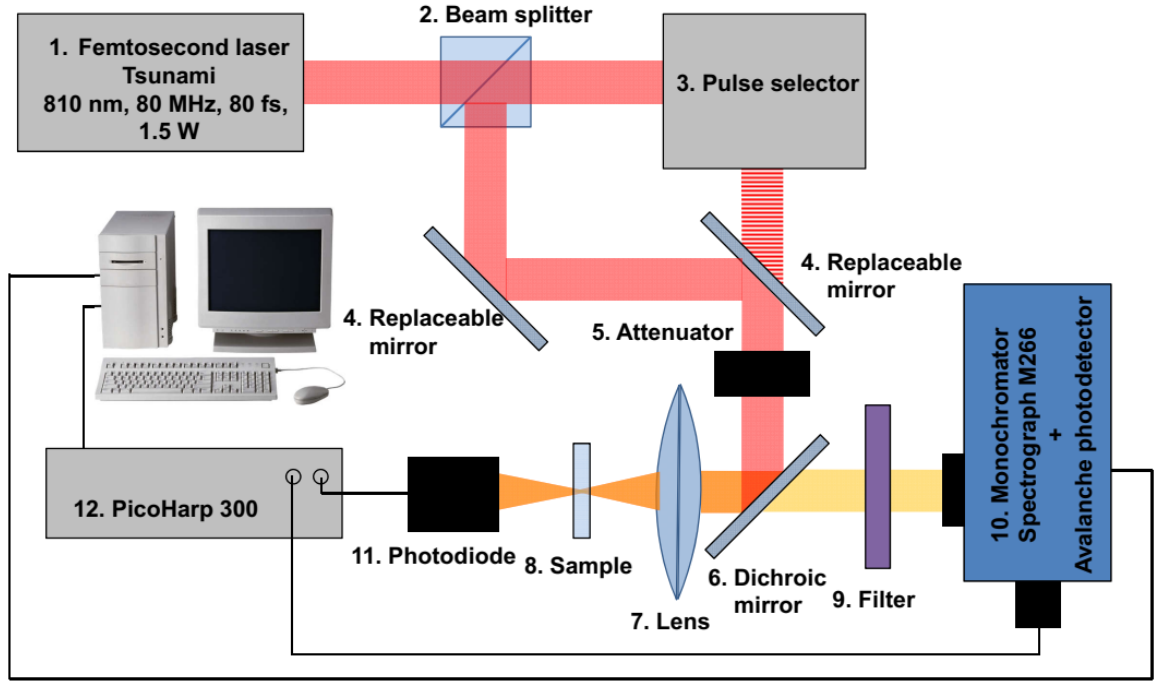
Fig. S3. Scheme of the experimental setup for measuring two-photon-excited photoluminescence.

The PL decay kinetics of some samples in this study were not monoexponential; therefore, for calculating the mean PL decay time, the kinetics was approximated by a multiexponential function of the form

$$I(t) = \sum A_i e^{-t/\tau_i}, \tag{S1}$$

where A_i and τ_i are constants obtained from the approximation, the first of which characterizes the contribution of the ith component, and the second, its decay time. The approximation was carried out using the least squares method according to the Levenberg–Marquardt algorithm. The main index that quantitatively characterized the temporal parameters of the PL signal was the average photoluminescence lifetime weighted by the number of emitted photons (intensity weighted average lifetime – τ_{lum}):

$$\tau_{lum} = \frac{\sum A_i \tau_i^2}{\sum A_i \tau_i}. \tag{S2}$$
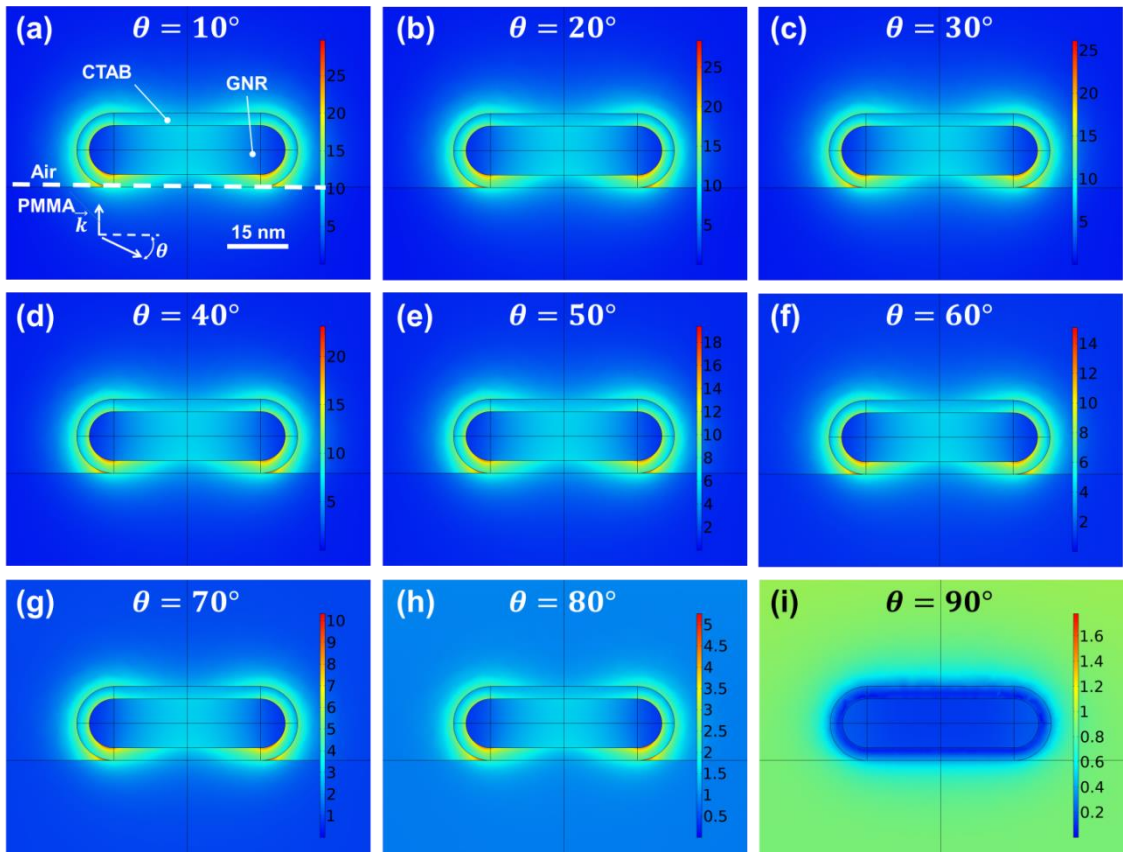
3. GNR-field simulations

Fig. S4. Near-field distribution for the GNR interacting with plane linearly polarized plane wave for different angles between GNR main axis and the field vector of wave: (a) 10°; (b) 20°; (c) 30°; (d) 40°; (e) 50°; (f) 60°; (g) 70°; (h) 80°; (i) 90°.
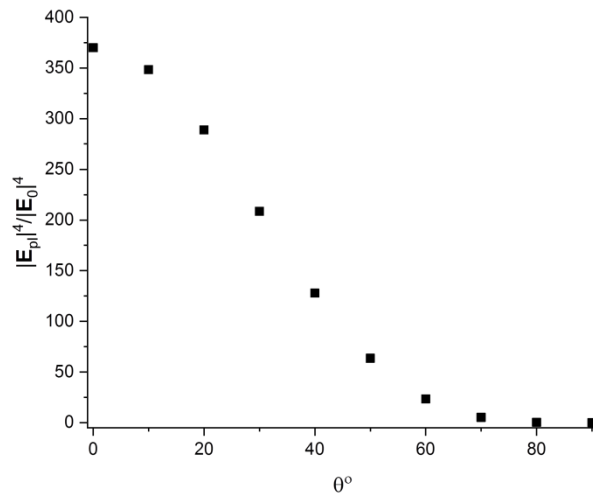

Fig. S5. Calculated dependence of the $|E_{pl}|^4/|E_0|^4$ averaged over the 20 nm-thick volume under GNR on the angle between GNR main axis and E_0 polarization.

References

[S1]   P. Samokhvalov, P. Linkov, J. Michel, M. Molinari, I. Nabiev, *Proc. SPIE* **2014**, *8955*, 89550S.

[S2]   J. Jasieniak, L. Smith, J. Van Embden, P. Mulvaney, M. Califano, *J. Phys. Chem. C* **2009**, *113*, 19468.

[S3]   J. J. Li, Y. A. Wang, W. Guo, J. C. Keay, T. D. Mishima, M. B. Johnson, X. Peng, J. *Am. Chem. Soc.* **2003**, *125*, 12567.